PROCEEDINGS OF SCIENCE

A new evaluation of the hadronic vacuum polarisation contributions to the muon $g-2$ and $\alpha(m_Z^2)$

Zhiqing Zhang[*†]
Laboratoire de l'Accélérateur Linéaire, IN2P3-CNRS et Univ. Paris-Sud 11, Univ. Paris-Saclay, 91898, Orsay Cedex, France
E-mail: zhangzq@lal.in2p3.fr

The hadronic vacuum polarisation contributions to the muon magnetic anomaly and to the running of the electromagnetic coupling constant at the Z-boson mass are reevaluated. Newest $e^+e^- \to$ hadrons cross-section data are included together with a phenomenological fit of the $\pi^+\pi^-$ threshold region in the evaluation of the dispersion integrals. The precision in the individual datasets cannot be fully exploited due to discrepancies that lead to additional systematic uncertainty in particular between BABAR and KLOE data in the dominant $\pi^+\pi^-$ channel. For the muon $(g-2)/2$, the lowest-order hadronic contribution obtained is $(693.9 \pm 4.0) \cdot 10^{-10}$. The full Standard Model prediction differs by 3.3σ from the experimental value. The five-quark hadronic contribution to $\alpha(m_Z^2)$ is evaluated to be $(276.1 \pm 1.0) \cdot 10^{-4}$.

European Physical Society Conference on High Energy Physics - EPS-HEP2019 - 10-17 July, 2019
Ghent, Belgium

[*]Speaker.
[†]in collaboration with M. Davier, A. Hoecker and B. Malaescu.

© Copyright owned by the author(s) under the terms of the Creative Commons Attribution-NonCommercial-NoDerivatives 4.0 International License (CC BY-NC-ND 4.0).

PoS(EPS-HEP2019)514

A new evaluation of the lowest-order hadronic vacuum polarisation (HVP) contribution, $a_\mu^{\rm had,LO}$, to the muon magnetic anomaly, and the hadronic contribution, $\Delta\alpha_{\rm had}(m_Z^2)$, to the running $\alpha(m_Z^2)$ at the Z-boson mass is presented. [1] The HVP contributions are currently the limiting factor on the prediction side for testing the Standard Model (SM) at quantum level by comparing the SM prediction of a_μ and the corresponding measurement, where a discrepancy over 3 standard deviations is observed [1]. With respect to our previous evaluation [2], the main new inputs and changes are listed here:

- For the dominant $\pi^+\pi^-$ channel, updated (new) cross-section measurements from KLOE [3] (CLEO [4]) are included. In addition, a phenomenological fit to supplement less precise data in the low-energy domain up to 0.6 GeV is performed.
- A new cross-section measurement from CMD-3 [14] of the K^+K^- channel, which provides third most important contribution after that of $\pi^+\pi^-$ and $\pi^+\pi^-\pi^0$ channels, is included.
- There are a few other new measurements in the $\pi^-\gamma$, $\pi^+\pi^-2\pi^0$, $\pi^+\pi^-3\pi^0$, $\eta\pi^+\pi^-$, $\eta\pi^+\pi^-\pi^0$, $\phi\eta$ and $K_SK_L\pi^0$ channels. A complete list is given in Ref. [1].
- Another important change is the introduction of an additional systematic uncertainty to account for a global discrepancy between $\pi^+\pi^-$ data from BABAR and KLOE, the two most precise measurements in this channel.

The phenomenological fit is performed to all pion form factor data using the relation:

$$\sigma^{(0)}(e^+e^-\to\pi^+\pi^-)=\frac{\pi\alpha^2}{3s}\beta_0^3(s)\cdot|F_\pi^0(s)|^2\cdot{\rm FSR}(s)\,, \tag{1}$$

where $\sigma^{(0)}$ is the bare cross section, α the fine structure constant, $\beta_0(s)=\sqrt{1-4m_\pi^2/s}$ is a threshold kinematic factor and ${\rm FSR}(s)$ is the final state radiation contribution. The pion form factor is an analytic function of s in the complex plane, except on the real axis above $4m_\pi^2$. It can be parameterised as a product of two functions [6]

$$F_\pi^0=G(s)\cdot J(s) \tag{2}$$

with

$$G(s)=1+\alpha_V s+\frac{\kappa s}{m_\omega^2-s-im_\omega\Gamma_\omega}\,, \tag{3}$$

and

$$J(s)=e^{1-\delta_1(s_0)/\pi}\cdot\left(1-\frac{s}{s_0}\right)^{\left[1-\frac{\delta_1(s_0)}{\pi}\right]\frac{s_0}{s}}\left(1-\frac{s}{s_0}\right)^{-1}\cdot\exp\left(\frac{s}{\pi}\int_{4m_\pi^2}^{s_0}dt\,\frac{\delta_1(t)}{t(t-s)}\right), \tag{4}$$

exploiting the unitarity constraint which identifies $\arg(F_\pi^0)$ with the P-wave $\pi^+\pi^-$ phase shift $\delta_1(s)$. The last term in Eq. (3) accounts for the $\omega\to\pi^+\pi^-$ contribution. The function $J(s)$ is taken from Refs. [7, 8]. Owing to ρ dominance, the phase shift $\delta_1(s)$ can be parameterised by [9]

$$\cot\delta_1(s)=\frac{\sqrt{s}}{2k^3(s)}\left(m_\rho^2-s\right)\left(\frac{2m_\pi^3}{m_\rho^2\sqrt{s}}+B_0+B_1\omega(s)\right) \tag{5}$$

[1] At the conference, preliminary results were presented. The final results are now available in [1] and briefly described here.

PoS(EPS-HEP2019)514

with

$$k(s) = \frac{\sqrt{s-4m_\pi^2}}{2}, \quad \omega(s) = \frac{\sqrt{s}-\sqrt{s_0-s}}{\sqrt{s}+\sqrt{s_0-s}}.$$

The six free parameters α_V, κ, m_ω, m_ρ, B_0 and B_1 are determined by the fit to the $\pi^+\pi^-$ data restricted to the region up to 1 GeV to stay below the threshold of significant inelastic channels. The width of the ω resonance is fixed to 8.49 MeV [10], and $\sqrt{s_0} = 1.05\,\text{GeV}$.

The result of the fit is compared in Fig. 1 (left) with the combined data obtained using the program library HVPTools [11]. In case of a local discrepancy among datasets, the uncertainty of each dataset is rescaled according to the local χ^2 value and number of degrees of freedom following the PDG prescription [10]. In the energy range between 0.3 and 0.6 GeV, the result of the fit yields for $a_\mu^{\text{had,LO}}[\pi\pi]$ a contribution of $109.8 \pm 0.4 \pm 0.4$ [2], where the first error is experimental and the second the model uncertainty. The latter is obtained by adding linearly the absolute values of following two variations: vary $\sqrt{s_0}$ to 1.3 GeV and remove the linear term $B_1\omega(s)$ from Eq.(5) since the resulting value of B_1 from the nominal fit is consistent with zero. The fit agrees with but is more precise than the result from the direct data integration of 109.6 ± 1.0.

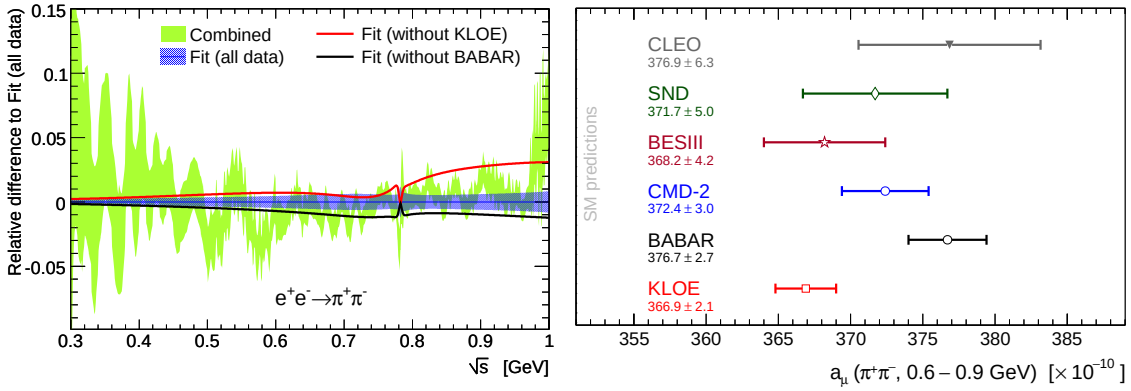

Figure 1: Left: The HVPTools combination (green band) relative to the result of the fit to all individual $\pi^+\pi^-$ data (blue band) versus centre-of-mass energy. The black and red curves show the results of two alternative fits where the data from KLOE and BABAR, respectively, were excluded. Right: Comparison of results for $a_\mu^{\text{had,LO}}[\pi\pi]$, evaluated between 0.6 GeV and 0.9 GeV for the various experiments. In case of CMD-2 and KLOE, all available measurements from these experiments have been combined using HVPTools.

In Fig. 1 (left), two alternative fits are compared. They correspond to the cases where, respectively, the BABAR and KLOE data are excluded from the fits. It clearly shows that these fit results do not agree with each other nor with the default fit result when all the data are used. The disagreement can also be seen in Fig. 1 (right) for $a_\mu^{\text{had,LO}}[\pi\pi]$ based on data integration between 0.6 and 0.9 GeV. In light of this discrepancy, which is not fully captured by the local uncertainty rescaling procedure, we add as an extra systematic uncertainty half of the full difference between the complete integrals without BABAR and KLOE, respectively, and we place the central value of the $a_\mu^{\text{had,LO}}[\pi\pi]$ contribution half-way between the two results. This procedure results in a total

[2] If not stated otherwise, all numerical results for a_μ are quoted in units of 10^{-10}.

PoS(EPS-HEP2019)514

$\pi^+\pi^-$ contribution of $a_\mu^{\mathrm{had,LO}}[\pi\pi] = 507.8 \pm 0.8 \pm 3.2$, where the first uncertainty is statistical and the second systematic (dominated by the new uncertainty of 2.8).

Tensions among datasets are also present in the K^+K^- channel. Figure 2 (left) shows a comparison of available measurements on the $\phi(1020)$ resonance. Previously, a 5.1% difference between CMD-2 [12] at VEPP-2M and BABAR [13], with the CMD-2 data being lower, was observed. New results from CMD-3 at VEPP-2000 [14] exhibit the opposite effect: they are 5.5% higher than BABAR. The discrepancy of almost 11% between the two CMD-2/3 datasets, which largely exceeds the quoted systematic uncertainty of 2.2%, of which only 1.2% accounts for uncertainties in the detection efficiency, is claimed to originate from a better understanding of the detection efficiency of low-energy kaons in the CMD-3 data.[3] Given the yet unresolved situation, both CMD-2 and CMD-3 datasets are kept, which, owing to the uncertainty rescaling procedure in presence of discrepancies, leads to a deterioration of the precision (by about a factor of 2) of the combined data (Fig. 2 (right)).

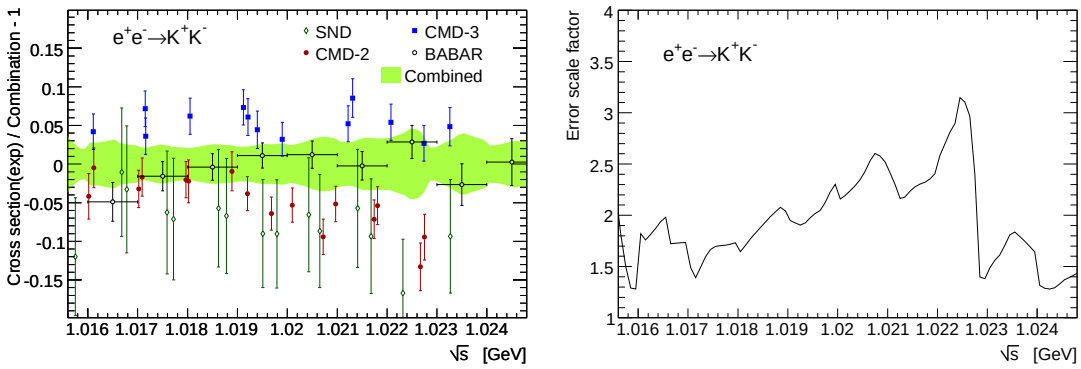

Figure 2: Left: comparison between individual $e^+e^- \to K^+K^-$ cross-section measurements from CMD-2 [12], BABAR [13], CMD-3 [14] and SND [15], and the HVPTools combination. Right: local scale factor versus centre-of-mass energy applied to the combined K^+K^- cross-section uncertainty to account for inconsistency in the individual measurements.

Among a total number of 32 exclusive channels considered for energies below 1.8 GeV, there are a few other updates but the resulting changes are very small (see Ref. [1]). Owing to new measurements, only very small contributions rely on estimates using isospin symmetry. The main changes together with the total LO HVP contribution with respect to our previous evaluation are shown in Table 1. The discrepancy between different datasets is now a limiting factor to further improve the precision of the LO HVP evaluation.

Adding to $a_\mu^{\mathrm{had,LO}}$ the contributions from higher order hadronic loops (see Ref. [1] for a full list of references cited therein), -9.87 ± 0.09 (NLO) and 1.24 ± 0.01 (NNLO), hadronic light-by-light scattering, 10.5 ± 2.6, as well as QED, $11\,658\,471.895 \pm 0.008$, and electroweak effects, 15.36 ± 0.10, one obtains the complete SM prediction $a_\mu^{\mathrm{SM}} = 11\,659\,183.0 \pm 4.0 \pm 2.6 \pm 0.1\ (4.8_{\mathrm{tot}})$, where the uncertainties account for lowest and higher order hadronic, and other contributions, respectively. The SM prediction deviates from the experimental value, $a_\mu^{\mathrm{exp}} = 11\,659\,209.1 \pm 5.4 \pm 3.3$ [16, 17], by 26.1 ± 7.9 (3.3σ). A compilation of recent SM predictions for a_μ compared with

[3] In comparison with the CMD-2/3 and SND measurements, the ISR method of BABAR benefits from higher-momentum kaons with better detection efficiency owing to the boost of the final state.

PoS(EPS-HEP2019)514

Channel	$a_\mu^{\mathrm{had,LO}}$ $[10^{-10}]$ 2019	$a_\mu^{\mathrm{had,LO}}$ $[10^{-10}]$ 2017	$\delta a_\mu^{\mathrm{had,LO}}$ change
$\pi^+\pi^-$	$507.80 \pm 0.83 \pm 3.19 \pm 0.60$	$507.14 \pm 1.13 \pm 2.20 \pm 0.75$	+30%
K^+K^-	$23.08 \pm 0.20 \pm 0.33 \pm 0.21$	$22.81 \pm 0.24 \pm 0.28 \pm 0.17$	+8%
Missing (%)	0.016 ± 0.016	0.09 ± 0.02	
Sum	$693.9 \pm 1.0 \pm 3.4 \pm 1.6 \pm 0.1_\psi \pm 0.7_{\mathrm{QCD}}$	$693.1 \pm 1.2 \pm 2.6 \pm 1.7 \pm 0.1_\psi \pm 0.7_{\mathrm{QCD}}$	+16%

Table 1: Comparison of the new evaluation with our previous one and their relative uncertainty change. Where three (or more) uncertainties are given, the first is statistical, the second channel-specific systematic, and the third common systematic, which is correlated with at least one another channel. The uncertainty in the Breit-Wigner integrals of the narrow resonances J/ψ and $\psi(2S)$ is dominated by the the respective electronic width measurements [10]. The QCD uncertainty includes effects from the α_s uncertainty, the truncation of the perturbative series at four loops, the FOPT vs. CIPT ambiguity, and quark mass uncertainties.

the experimental result is given in Fig. 3. To go beyond the current non-conclusive discrepancy between the SM prediction and the measurement, much more precise cross-section measurements on the prediction side are needed since there is a good perspective in the near future for a significant uncertainty reduction on the measurement from the Fermilab experiment.

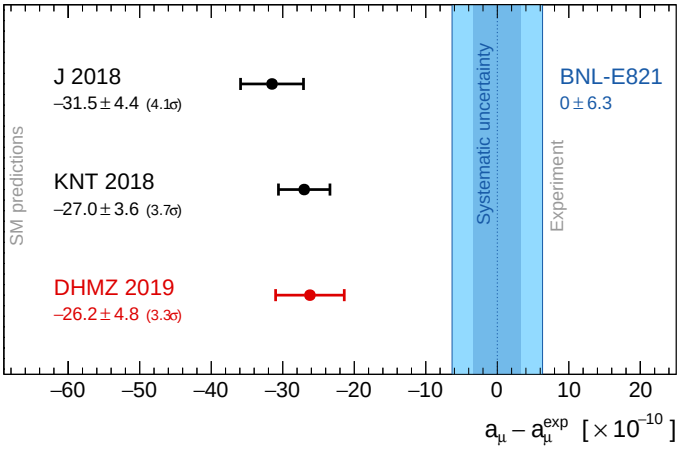

Figure 3: Compilation of recent data-driven results for a_μ^{SM} (in units of 10^{-10}), subtracted by the central value of the experimental average [16, 17]. The blue vertical band indicates the experimental uncertainty, with the darker inlet representing the experimental systematic uncertainty. The representative SM predictions are taken from KNT 2018 [18], J 2018 [19], and this work (DHMZ 2019).

The corresponding result for the hadronic contribution to the running of $\alpha(m_Z^2)$ is $\Delta\alpha_{\mathrm{had}}(m_Z^2) = (275.4 \pm 1.0) \cdot 10^{-4}$, the uncertainty of which is dominated by data systematic effects $(0.7 \cdot 10^{-4})$ and the uncertainty in the QCD prediction $(0.6 \cdot 10^{-4})$. The result without the new BABAR/KLOE systematic uncertainty is 275.3 ± 0.9. Adding to this the four-loop leptonic contribution, $\Delta\alpha_{\mathrm{lep}}(m_Z^2) = (314.979 \pm 0.002) \cdot 10^{-4}$, one finds $\alpha^{-1}(m_Z^2) = 128.946 \pm 0.013$. The current uncertainty on $\alpha(m_Z^2)$ is sub-dominant in the SM prediction of the W-boson mass (the dominant uncertainties are due to the top mass and of theoretical origin), but dominates the prediction of $\sin^2\theta_{\mathrm{eff}}^{\ell}$, which, however, is about twice more accurate than the combination of all present measurements.

PoS(EPS-HEP2019)514

References

[1] M. Davier, A. Hoecker, B. Malaescu and Z. Zhang, arXiv:1908.00921 [hep-ph].

[2] M. Davier, A. Hoecker, B. Malaescu and Z. Zhang, Eur. Phys. J. C **77** (2017) no.12, 827 doi:10.1140/epjc/s10052-017-5161-6 [arXiv:1706.09436 [hep-ph]].

[3] A. Anastasi *et al.* [KLOE-2 Collaboration], JHEP **1803** (2018) 173 doi:10.1007/JHEP03(2018)173 [arXiv:1711.03085 [hep-ex]].

[4] T. Xiao, S. Dobbs, A. Tomaradze, K. K. Seth and G. Bonvicini, Phys. Rev. D **97** (2018) no.3, 032012 doi:10.1103/PhysRevD.97.032012 [arXiv:1712.04530 [hep-ex]].

[5] E. A. Kozyrev *et al.*, Phys. Lett. B **779** (2018) 64 doi:10.1016/j.physletb.2018.01.079 [arXiv:1710.02989 [hep-ex]].

[6] C. Hanhart, S. Holz, B. Kubis, A. Kupść, A. Wirzba and C.W. Xiao, Eur. Phys. J. C 77, 98 (2017) Erratum: [Eur. Phys. J. C 78, 450 (2018)] [arXiv:1611.09359].

[7] J.F. De Troconiz and F.J. Yndurain, Phys. Rev. D 65, 093001 (2002) [hep-ph/0106025].

[8] J.F. de Troconiz and F.J. Yndurain, Phys. Rev. D 71, 073008 (2005) [hep-ph/0402285].

[9] R. Garcia-Martin, R. Kaminski, J.R. Pelaez, J. Ruiz de Elvira and F.J. Yndurain, Phys. Rev. D 83, 074004 (2011) [arXiv:1102.2183].

[10] Particle Data Group, Phys. Rev. D 98, 030001 (2018) and 2019 update. http://pdglive.lbl.gov.

[11] M. Davier, A. Hoecker, B. Malaescu, C.Z. Yuan, and Z. Zhang, Eur. Phys. J. C 66, 1 (2010) [arXiv:0908.4300].

[12] CMD-2 Collaboration, Phys. Lett. B 669, 217 (2008) [arXiv:0804.0178].

[13] BABAR Collaboration, Phys. Rev. D 88, 032013 (2013) [arXiv:1306.3600].

[14] E.A. Kozyrev *et al.*, Phys. Lett. B 779, 64 (2018) [arXiv:1710.02989].

[15] SND Collaboration, Phys. Rev. D 94, 112006 (2016) [arXiv:1608.08757].

[16] Muon *g*–2 Collaboration, Phys. Rev. D 73, 072003 (2006) [hep-ex/0602035].

[17] A. Hoecker and W. Marciano, "The Muon Anomalous Magnetic Moment", in: Review of Particle Physics, Particle Data Group, Phys. Rev. D 98, 030001 (2018).

[18] A. Keshavarzi, D. Nomura and T. Teubner, Phys. Rev. D 97, 114025 (2018) [arXiv:1802.02995].

[19] F. Jegerlehner, EPJ Web of Conferences 166, 00022 (2018) [arXiv:1705.00263].

PoS(EPS-HEP2019)514